HELIUM-BEARING "VESICULAR" NANOPHASE METALLIC IRON PARTICLES IN LUNAR REGOLITH GRAINS. B. A. Cymes[1], K. D. Burgess[2], R. M. Stroud[2], and The ANGSA Science Team, [1]NRC Postdoctoral Research Associate, U.S. Naval Research Laboratory, Washington DC 20375 (brittany.cymes.ctr@nrl.navy.mil), [2]U.S. Naval Research Laboratory, Washington DC 20375.

Introduction: Space weathering refers to the physical and chemical changes occurring on the surfaces of airless bodies (e.g. the Moon, asteroids) in response to processes such as solar wind irradiation and micrometeorite bombardment. Over time, space weathering can alter the surfaces of individual regolith grains, producing thin (<200 nm) amorphous rims which can include vesicles, nanophase metallic iron particles ($npFe^0$), or a combination of these textures [1-3]. Although $npFe^0$ are considered to be a "final" product of space weathering, how they might evolve over time in response to continual weathering remains unconstrained. In this study, we describe identification of helium-bearing vesicular $npFe^0$ using scanning transmission electron microscopy (STEM) and electron energy loss spectroscopy (EELS). These powerful techniques allow for sub-nanometer imaging and microanalysis of individual space weathered grains and can reveal important sample features typically inaccessible with bulk-level approaches.

Methodology: We analyzed sub-45 µm fractions of Apollo 17 soils 79221 (mature), 72321 (mature), 72501 (mature), 76241 (submature), and 76261 (submature). Soil grains were prepared for STEM analysis by both ultramicrotome (UM) sectioning and by focused ion beam (FIB) microscopy. UM samples were prepared by embedding grains in epoxy and sectioning to ~100 nm with a diamond knife; the sections were supported on 3 mm lacey-carbon Cu TEM grids. FIB samples were prepared by dispersing soil grains onto C-tape adhered to an Al pin-stub and coated with ~80 nm of amorphous C. Individual grains were identified and prepared using an FEI Helios G3 Dual Beam FIB-SEM. The grains were first protected with ~1 µm of amorphous C and thinned to 1-2 µm with a 30 keV Ga^+ ion beam. After Pt-welding the sample to Cu TEM half-grids, the samples were thinned to electron transparency (80-100 nm). All samples were held under vacuum at ~20°C for 48 hrs to drive off adsorbed water before introduction into the UHV STEM environment. STEM data were acquired using an aberration-corrected Nion UltraSTEM200-X operated at 200 keV and 40 pA with a 0.1 nm probe. Images were acquired in density- and thickness-sensitive high angle annual dark field (HAADF) mode. EELS data were acquired with a Gatan Enfinium ER Dual EELS spectrometer as spectrum images (SI), in which a spectrum is acquired at each pixel in a given image, providing information about thickness variations, composition, and oxidation state. The He K-edge was deconvolved from the bulk plasmon using a multiple linear least squares (MLLS) fitting routine.

Results & Discussion: Vesicular $npFe^0$ (v-$npFe^0$) occur in all samples as spheroid or irregular-rounded particles with networks of void spaces (Fig. 1a). Particles typically occur in two size ranges: <15 nm and ~20-100 nm. Small v-$npFe^0$ often occur in association with large v-$npFe^0$ (Fig. 1a), but are also found alone (Fig. 1b). Multiple, discrete, large v-$npFe^0$ often occur in the same grain but can also appear as coalescing bodies (Fig. 1c). Small v-$npFe^0$ occur in the space weathered rims of multiple mineral phases (e.g. olivine, plagioclase), but large v-$npFe^0$ are found almost exclusively in agglutinitic glass grains.

Particles similar to v-$npFe^0$ have been previously noted in the literature. Hollow, oxidized npFe were described by Thompson et al. [4] in soil 15071 (submature) associated with oxidizing conditions in a glass matrix and in soil 71061 (immature) by Burgess et al. [5] in an amorphous silicate rim. Burgess et al. [5] also describe surface-correlated 'pitted' $npFe^0$ in an agglutinate glass in 79221 which are similar in morphology and occurrence to the v-$npFe^0$ we describe here.

Although particles with similar morphology have been observed, EELS-SI analyses reveal that many of the large v-$npFe^0$ we examined contain He (Fig. 1d-e). The He K-edge signal spatially correlates with the void spaces (Fig. 1e-inset), and thus He likely played a role in their formation. Helium is a main component of the solar wind and has been detected in space weathered chromite and ilmenite previously using EELS (e.g. [6]). Finding He within $npFe^0$ is important because, as a surface-correlated regolith component, $npFe^0$ may shed light on volatile emplacement and cycling within the regolith over time.

Solar wind-driven formation mechanism. Vesicle development in all space weathered materials is typically linked to solar-wind ion implantation rather than impact-related processes [e.g. 1-2]. A glass grain from soil 79221 supports a solar-wind driven formation mechanism for v-$npFe^0$. In this FIB sample, $npFe^0$ are dispersed throughout the volume of the grain, but only those within ~100 nm of the surface had vesicles (Fig. 2a). One v-$npFe^0$ found in the rim had vesicles only on the side facing the grain exterior (Fig. 2b), indicating that vesicles form within intact $npFe^0$ from outside processes. EELS-SI data show that this particle contains He within the vesicles (Fig. 2c). If v-$npFe^0$ development is driven by H^+ and He^+ implantation, we would assume those v-$npFe^0$ in which solar wind ions are not detected may have simply lost them through diffusion. Because our samples were submature-mature, v-$npFe^0$ may represent an advanced space-weathering product. Additional analysis of immature grains is needed to verify this.

An alternative formation mechanism. Although evidence for solar wind irradiation-driven formation of v-$npFe^0$ is strong, we have also found He-bearing v-$npFe^0$ in permanently-shaded soils 72321 and 76241. In these soils, solar wind irradiation may still have caused He-bearing $npFe^0$ development, but their formation would have been prior to emplacement of the shading boulders at the collection sites. However, because large, He-bearing v-$npFe^0$ are associated with agglutinitic glassy phases, another potential pathway may involve an impact-related heating process but additional data are needed to explore this possibility.

Conclusion: Vesicular nanophase metallic iron particles (v-$npFe^0$) have been identified in multiple Apollo 17 soils varying in maturity and exposure to the solar wind. Many large (~20-100 nm) v-$npFe^0$ contain pockets of solar wind-derived helium. A glass grain from soil 79221 contains $npFe^0$ throughout the volume of the grain but only those within ~100 nm of the grain edge contains vesicles and one v-$npFe^0$ has He-filled vesicles only on the side closest to the grain exterior, suggesting that development of v-$npFe^0$ is driven by ion implantation into particles formed by melt-driven processes. The identification of a “new” noble gas reservoir phase, $npFe^0$, is important as the metallic nanoparticles appear, similarly to oxide phases identified previously, to retain He more effectively than silicate minerals.

Acknowledgments: This work is supported by NASA Award 80HQTR19T0057 and SSERVI Award 80NSSC19M0215.

References: [1] Pieters, C. M. and Noble, S. K. (2016) *J. Geophys. Res.* **121**, 1865-1884. [2] Hapke, B. (2001) *J. Geophys. Res.* **106**, 10039-10073. [3] Keller, L. P. and McKay, D. S. (1997) *Geochim. Cosmochim. Acta* **61**, 2331-2341. [4] Thompson, M. S., Zega, T. J., Becerra, P., Keane, J. T., and Byrne, S. (2016) *Meteor. Planet. Sci.* **51**, 1082-1095. [5] Burgess, K. D. and Stroud, R. M. (2018) *J. Geophs. Res. Planet.* **123**, 2022-2037. [6] Burgess, K. D. and Stroud, R. M. (2018) *Geochim. Cosmochim. Acta.* **224**, 64-79.

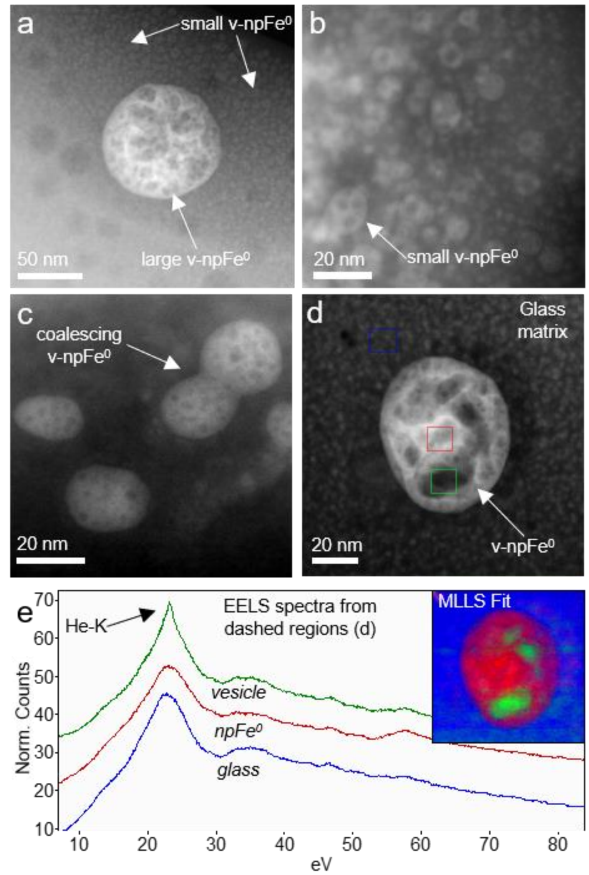

Figure 1. (a) HAADF-STEM image of a glass grain in soil 79221 with a 100 nm v-$npFe^0$ in association with a population of 3-8 nm v-$npFe^0$; **(b)** a glass grain in soil 76261 showing a population of 5-15 nm v-$npFe^0$; **(c)** an agglutinate glass grain from soil 76421 containing coalescing v-$npFe^0$; **(d)** a glass grain in soil 79221 showing a 60 nm v-$npFe^0$ where EELS-SI data were acquired; **(e)** Low-loss EELS-SI data from dashed areas in (d) showing He K-edge at ~22 eV compared to plasmons of $npFe^0$ and glass (inset: MLLS-fitting integral map of vesicle signal (green), npFe0 signal (red), and glass signal (blue).

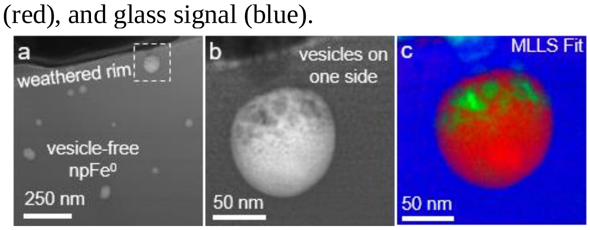

Figure 2. (a) HAADF-STEM image of a space weathered glass grain from sample 79221 bearing both v-$npFe^0$ near the grain surface and vesicle-free $npFe^0$ in the grain interior. **(b)** HAADF-STEM image of dashed inset of (a) showing detail of $npFe^0$ with vesicles on the side facing the grain exterior. **(c)** Results of MLLS fitting showing a map of He-K (green), the $npFe^0$ (red), and the surrounding glass (blue).